INTERNATIONAL JOURNAL OF ONCOLOGY 46: 99-106, 2015

# Autoacetylation regulates differentially the roles of ARD1 variants in tumorigenesis

JI HAE SEO[1], JI-HYEON PARK[1], EUN JI LEE[1], TAM THUY LU VO[1], HOON CHOI[1], JAE KYUNG JANG[1], HEE-JUN WEE[1], BUM JU AHN[1], JONG-HO CHA[1], MIN WOOK SHIN[1] and KYU-WON KIM[1,2]

[1]SNU-Harvard Neurovascular Protection Research Center, College of Pharmacy and Research Institute of Pharmaceutical Sciences, [2]Department of Molecular Medicine and Biopharmaceutical Sciences, Graduate School of Convergence Science and Technology, and College of Medicine or College of Pharmacy, Seoul National University, Seoul 151-742, Republic of Korea

Received May 6, 2014; Accepted June 27, 2014

DOI: 10.3892/ijo.2014.2708

**Abstract.** ARD1 is an acetyltransferase with several variants derived from alternative splicing. Among ARD1 variants, mouse ARD1$^{225}$ (mARD1$^{225}$), mouse ARD1$^{235}$ (mARD1$^{235}$), and human ARD1$^{235}$ (hARD1$^{235}$) have been the most extensively characterized and are known to have different biological functions. In the present study, we demonstrated that mARD1$^{225}$, mARD1$^{235}$, and hARD1$^{235}$ have conserved autoacetylation activities, and that they selectively regulate distinct roles of ARD1 variants in tumorigenesis. Using purified recombinants for ARD1 variants, we found that mARD1$^{225}$, mARD1$^{235}$, and hARD1$^{235}$ undergo similar autoacetylation with the target site conserved at the Lys136 residue. Moreover, functional investigations revealed that the role of mARD1$^{225}$ autoacetylation is completely distinguishable from that of mARD1$^{235}$ and hARD1$^{235}$. Under hypoxic conditions, mARD1$^{225}$ autoacetylation inhibited tumor angiogenesis by decreasing the stability of hypoxia-inducible factor-1α (HIF-1α). Autoacetylation stimulated the catalytic activity of mARD1$^{225}$ to acetylate Lys532 of the oxygen-dependent degradation (ODD) domain of HIF-1α, leading to the proteosomal degradation of HIF-1α. In contrast, autoacetylation of mARD1$^{235}$ and hARD1$^{235}$ contributed to cellular growth under normoxic conditions by increasing the expression of cyclin D1. Taken together, these data suggest that autoacetylation of ARD1 variants differentially regulates angiogenesis and cell proliferation in an isoform-specific manner.

## Materials and methods

*Reagents and antibodies*. Anti-HIF-1α antibody was purchased from BD Pharmingen. Anti-Myc and green fluorescent protein (GFP) antibodies were purchased from Santa Cruz Biotechnology. Anti-acetyl-lysine antibody was purchased from Cell Signaling. Anti-tubulin and Flag antibodies were purchased from Sigma-Aldrich. MG132 was purchased from Calbiochem.

*Cell culture and hypoxic condition*. HeLa cells and human umbilical vein endothelial cells (HUVECs) were grown in Dulbecco's modified Eagle's medium supplemented with 10% fetal bovine serum (FBS) and EBM-2 medium supplemented with growth factors (Lonza), respectively. Cells were maintained at 37˚C in a humidified atmosphere containing 5% $CO_2$. Hypoxic conditions were created by incubating cells at 37˚C in a chamber containing 5% $CO_2$, 1% $O_2$, and the remainder $N_2$.

*Plasmid construction and transfection*. To construct expression vectors for ARD1 variants, ARD1 cDNA was amplified by polymerase chain reaction (PCR) and subcloned into GFP- or Myc-tagged pCS2+ vectors for cell expression, and pGEX-4T for bacterial induction of the recombinant protein. Mutations in ARD1 were created using the Muta-Direct™ Site Directed Mutagenesis kit (Intron) according to the manufacturer's instructions. Cells were transfected with Lipofectamine (Life Technology) or Polyfect (Qiagen) according to the manufacturer's instructions.

*Immunoblotting and immunoprecipitation*. Cells were harvested and extracted in lysis buffer (10 mM HEPES at pH 7.9, 40 mM NaCl, 0.1 mM ethylenediaminetetraacetic acid (EDTA), 5% glycerol, 1 mM dithiothreitol (DTT), and protease inhibitors). The concentrations of the protein extracts were measured with the BCA assay. For immunoprecipitations, relevant primary antibodies were added to 1 mg of the protein extracts and incubated overnight at 4˚C. The immunoprecipitates and total cell lysates were resolved in sodium dodecyl-sulfate polyacrylamide gel electrophoresis gels and transferred onto nitrocellulose membranes (Amersham Pharmacia Bioscience). The membrane was probed with a primary antibody followed by a secondary antibody conjugated with horseradish peroxidase, and detected using an ECL system (Intron Biotechnology).

*In vitro acetylation assay*. Recombinants of GST-ARD1 variants were freshly prepared as described previously (11). These recombinants were incubated with or without His-tagged oxygen-dependent degradation (ODD) domain of HIF-1α recombinants in the reaction mixture (50 mM Tris-HCl at pH 8.0, 0.1 mM EDTA, 1 mM DTT, 10% glycerol, and 10 mM acetyl-CoA) at 37˚C.

*Reverse transcription (RT)-PCR analysis*. Total RNA was extracted using an RNA extraction kit (Invitrogen). cDNA was synthesized from 2 μg of RNA using an oligo(dT) primer. Primers used for PCR were as follows: human *VEGF*, 5'-GAGAATTCGGCCTCCGAAACCATGAACTT TCTGCT-3' (forward) and 5'-GAGCATGCCCTCCTGCCC GGCTCACCGC-3' (reverse); *ARD1*, 5'-ATGAACATCCGC AATGCGAG-3' (forward) and 5'-CTCATATCATGGCT CGAGAGG-3' (reverse); *cyclin D1*, 5'-CTGGCCATGAA CTACCTGGA-3' (forward) and 5'-GTCACACTTGATCAC TCTGG-3' (reverse); *GAPDH*, 5'-ACCACAGTCCATGCCAT CAC-3' (forward) and 5'-TCCACCACCCTGTTGCTGTA-3' (reverse). The PCR amplification was carried out for 25 cycles with *ARD1*, *cyclin D1*, and *GAPDH*, and for 30 cycles with *VEGF*.

*Tube formation assay*. For the tube formation assay, 24-well plates were coated with Matrigel (BD Biosciences) and allowed to polymerize at 37˚C for 30 min. HUVECs were seeded ($5x10^4$ cells per well) onto Matrigel with 500 μl conditioned medium from HeLa cells. Tube formation was assessed after 4 h and quantified by determining the number of rings.

*Cell proliferation assay*. The cell growth rate was measured using a non-radioactive proliferation assay kit (Promega) according to the manufacturer's instructions. Briefly, cells were plated on 96-well plates and grown for 3 days. Substrate solution (20 μl) was then added and the cells were incubated for 1 h to allow color development. The absorbance at 492 nm was measured as an index of the number of proliferating cells.

*Statistical analysis*. Results are presented as means ± SD, and P-values were calculated by applying the two-tailed Student's t-test to data from three independent experiments. Differences were considered statistically significant when $P<0.05$.

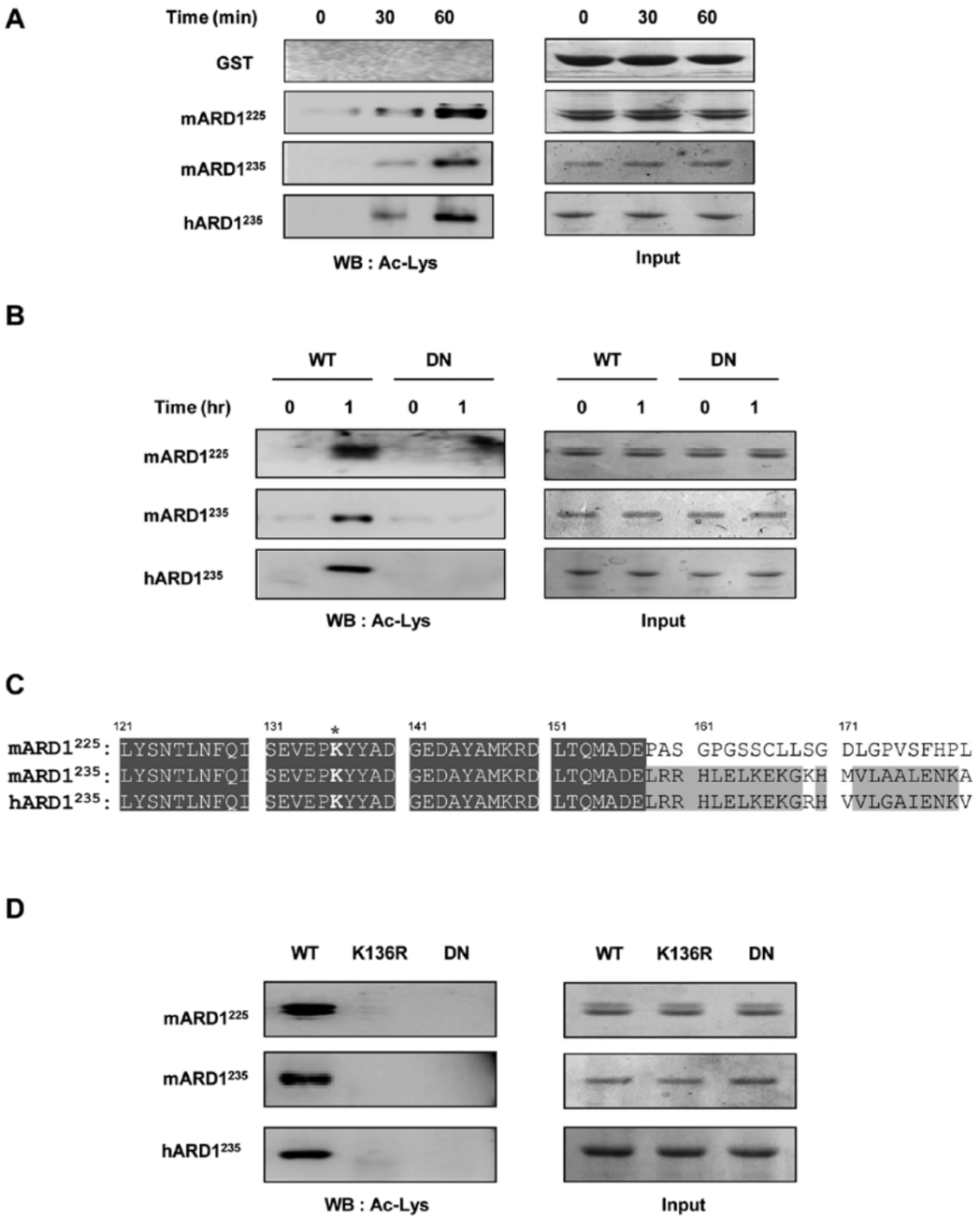


Figure 1. ARD1 variants self-acetylate the K136 residue *in vitro*. (A) Purified recombinants for GST-mARD1$^{225}$, GST-mARD1$^{235}$, and GST-hARD1$^{235}$ were subjected to the *in vitro* acetylation assay for 30 and 60 min. Purified GST recombinant was subjected to the acetylation assay under the same conditions as a control. Acetylated proteins were detected by an anti-acetyl lysine (Ac-Lys) antibody. Total proteins were stained with Coomassie Brilliant Blue (input). (B) Wild-type GST-ARD1 recombinants (WT) and dominant negative GST-ARD1 (DN) with no catalytic activity were subjected to the *in vitro* acetylation assay. Acetylation status was analyzed with Ac-Lys antibody. Total proteins were stained with Coomassie Brilliant Blue (input). (C) The amino acid sequences of the ARD1 variants were compared. The conserved autoacetylation target site of ARD1 variants is indicated by an asterisk (*). (D) Purified GST recombinants of wild-type ARD1 (WT), K136R mutant ARD1 (K136R), and dominant negative ARD1 (DN) were subjected to the *in vitro* acetylation assay for 1 h, followed by western blot analysis with Ac-Lys antibody. Total proteins were stained with Coomassie Brilliant Blue (input).

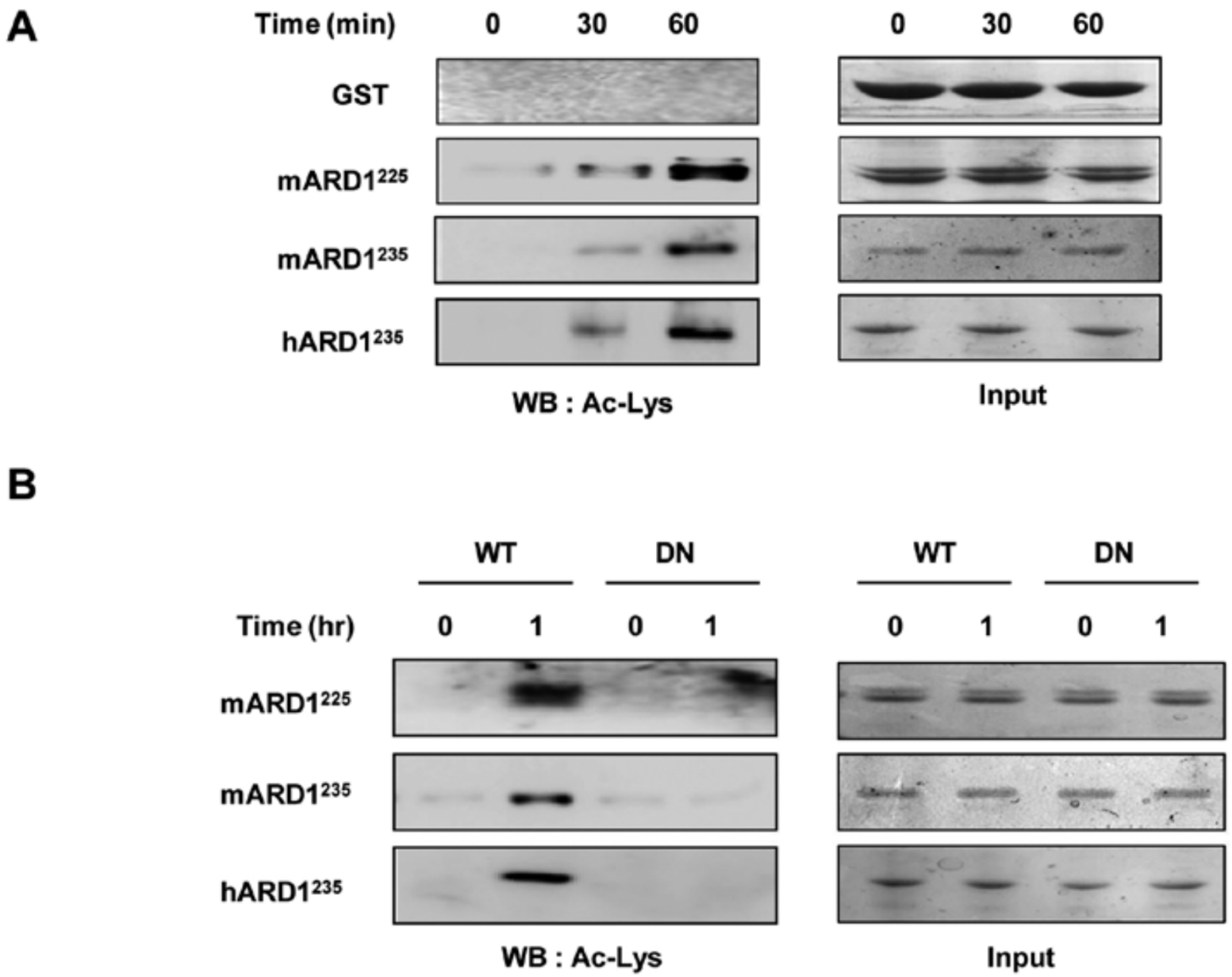
A
Time (min)
0
30
60
0
30
60
GST
mARD1225
mARD1235
hARD1235
WB : Ac-Lys
Input
B
WT
DN
WT
DN
Time (hr)
0
1
0
1
0
1
0
1
mARD1225
mARD1235
hARD1235
WB : Ac-Lys
Input

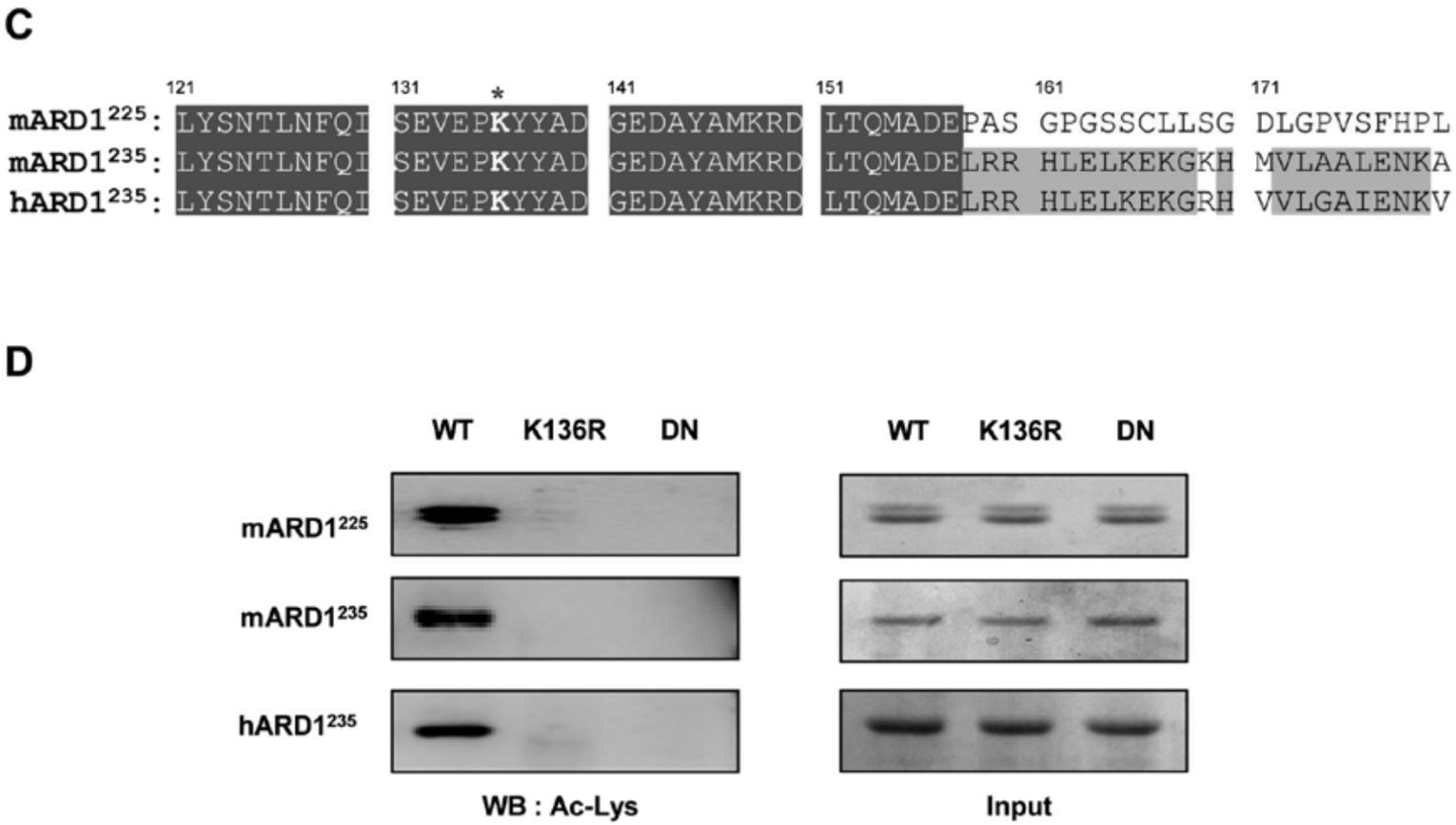


Figure 1. ARD1 variants self-acetylate the K136 residue *in vitro*. (A) Purified recombinants for GST-mARD1$^{225}$, GST-mARD1$^{235}$, and GST-hARD1$^{235}$ were subjected to the *in vitro* acetylation assay for 30 and 60 min. Purified GST recombinant was subjected to the acetylation assay under the same conditions as a control. Acetylated proteins were detected by an anti-acetyl lysine (Ac-Lys) antibody. Total proteins were stained with Coomassie Brilliant Blue (input). (B) Wild-type GST-ARD1 recombinants (WT) and dominant negative GST-ARD1 (DN) with no catalytic activity were subjected to the *in vitro* acetylation assay. Acetylation status was analyzed with Ac-Lys antibody. Total proteins were stained with Coomassie Brilliant Blue (input). (C) The amino acid sequences of the ARD1 variants were compared. The conserved autoacetylation target site of ARD1 variants is indicated by an asterisk (*). (D) Purified GST recombinants of wild-type ARD1 (WT), K136R mutant ARD1 (K136R), and dominant negative ARD1 (DN) were subjected to the *in vitro* acetylation assay for 1 h, followed by western blot analysis with Ac-Lys antibody. Total proteins were stained with Coomassie Brilliant Blue (input).

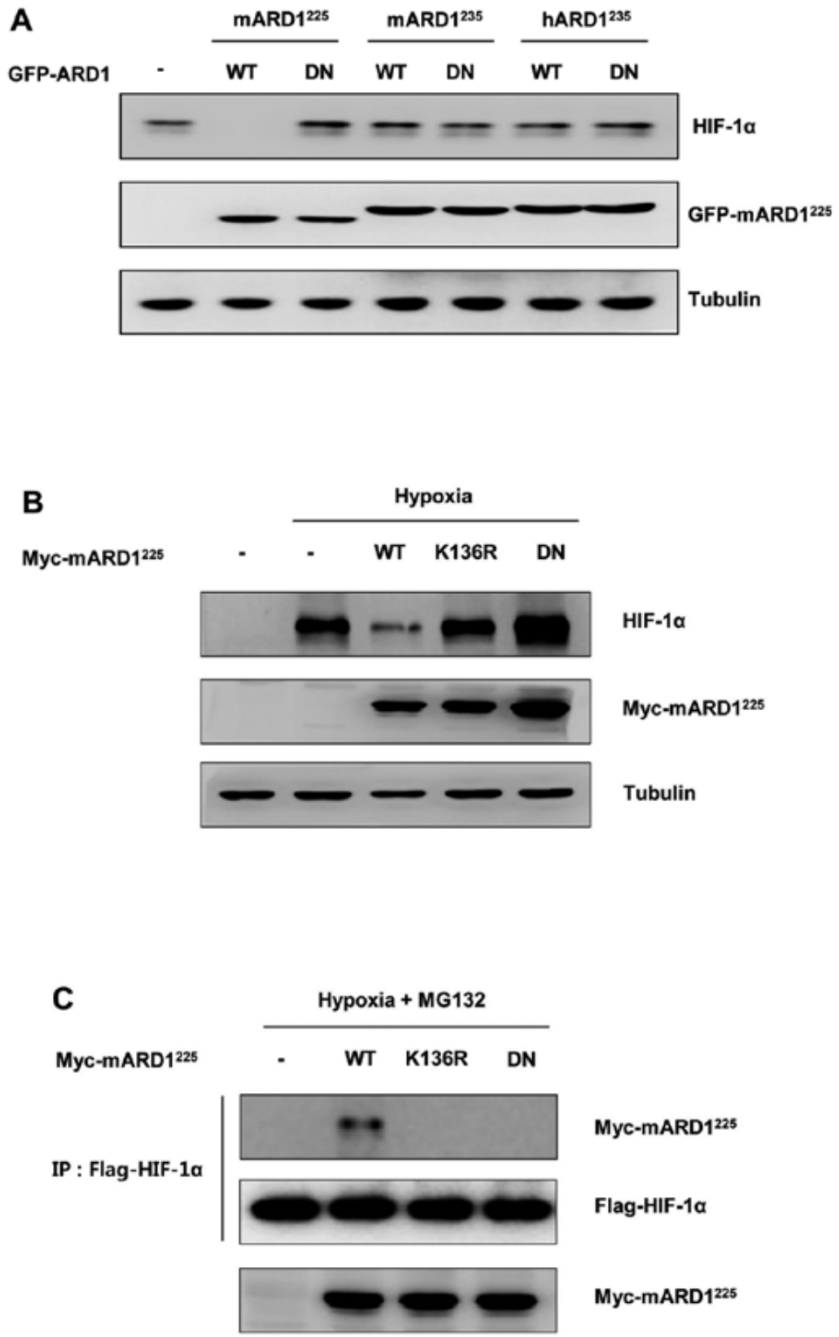


Figure 2. Autoacetylation of mARD1$^{225}$ decreases the stability of HIF-1α protein. (A) HeLa cells were transfected with plasmids encoding GFP-tagged wild-type ARD1 (WT) or dominant negative ARD1 (DN), then incubated under hypoxic conditions for 4 h. Total cell extracts were subjected to western blot analysis with anti-HIF-1α, anti-GFP, and anti-tubulin antibodies. (B) Myc-tagged plasmids for wild-type mARD1$^{225}$ (WT), K136R mutant mARD1$^{225}$ (K136), and dominant negative mARD1$^{225}$ (DN) were transiently expressed in HeLa cells. HIF-1α protein levels were analyzed by western blot analysis. (C) After transfection of HeLa cells with Flag-tagged HIF-1α and Myc-tagged mARD1$^{225}$ plasmids, cells were treated with 10 $\mu$M MG132 for 4 h under hypoxic conditions. Total cell lysates were immunoprecipitated with an anti-Flag antibody. The presence of Myc-mARD1$^{225}$ in the immunoprecipitates was examined with an anti-Myc antibody. Immunoprecipitated HIF-1α protein and total cell extracts were analyzed with anti-HIF-1α and anti-Myc antibodies, respectively.

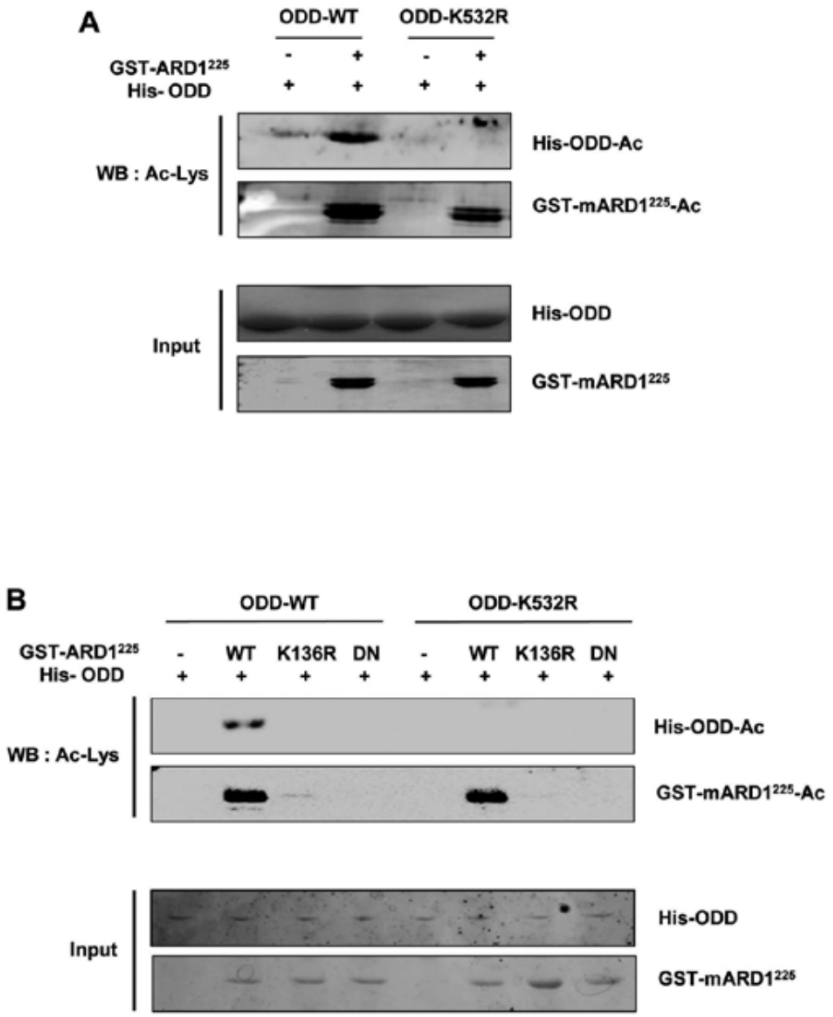


Figure 3. Autoacetylation of mARD1$^{225}$ is required for HIF-1α acetylation. (A) Wild-type HIF-1α ODD recombinant (ODD-WT) and K532R mutant HIF-1α ODD recombinant (ODD-K532R) were purified and subjected to the *in vitro* acetylation assay for 1 h with or without mARD1$^{225}$. Acetylation was analyzed by western blot analysis using an anti-Ac-Lys antibody. Total proteins were stained with Coomassie Brilliant Blue (input). (B) Purified GST-tagged recombinants of wild-type mARD1$^{225}$ (WT), K136R mutant mARD1$^{225}$ (K136R), and dominant negative mARD1$^{225}$ (DN) were subjected to the *in vitro* acetylation assay with His-tagged ODD-WT or ODD-K532R recombinants. Acetylated proteins were detected using Ac-Lys antibody and total proteins were stained with Coomassie Brilliant Blue (input).

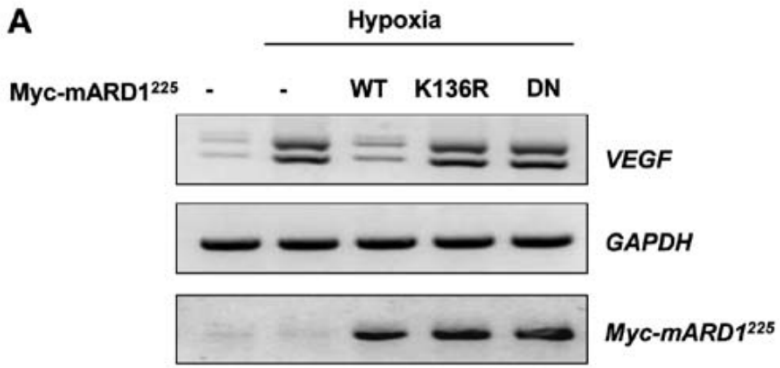


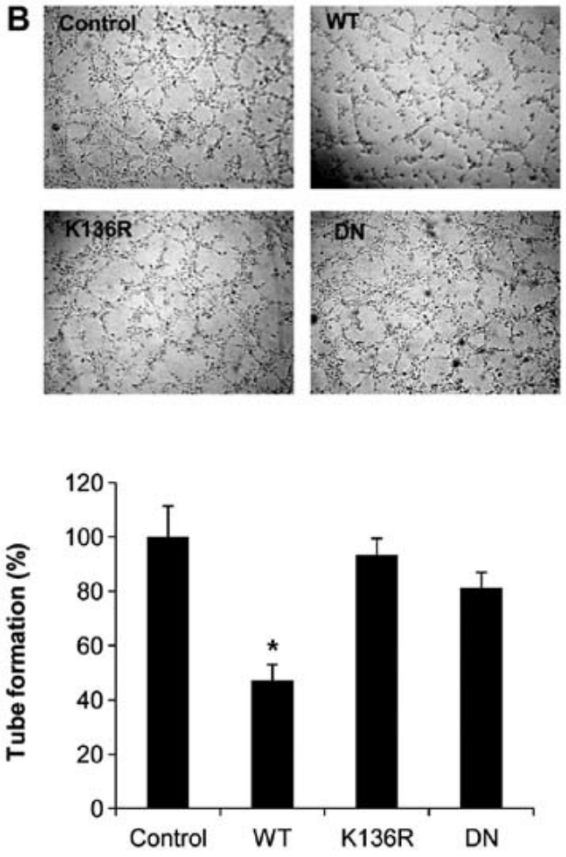


Figure 4. Autoacetylation of mARD1$^{225}$ inhibits angiogenesis. (A) HeLa cells were transfected with Myc-tagged mARD1$^{225}$ plasmids and incubated under hypoxic conditions for 24 h. Total RNA was extracted for RT-PCR analysis. Expression of *VEGF* and *GAPDH* mRNA was determined using specific primers. (B) HeLa cells expressing the mARD1$^{225}$ plasmids were incubated under hypoxic conditions for 24 h and conditioned media were collected. Human umbilical vein endothelial cells (HUVECs) were treated with conditioned media for 4 h. Tube formation was photographed and quantified by counting the number of rings. $^{*}P<0.05$ versus control.

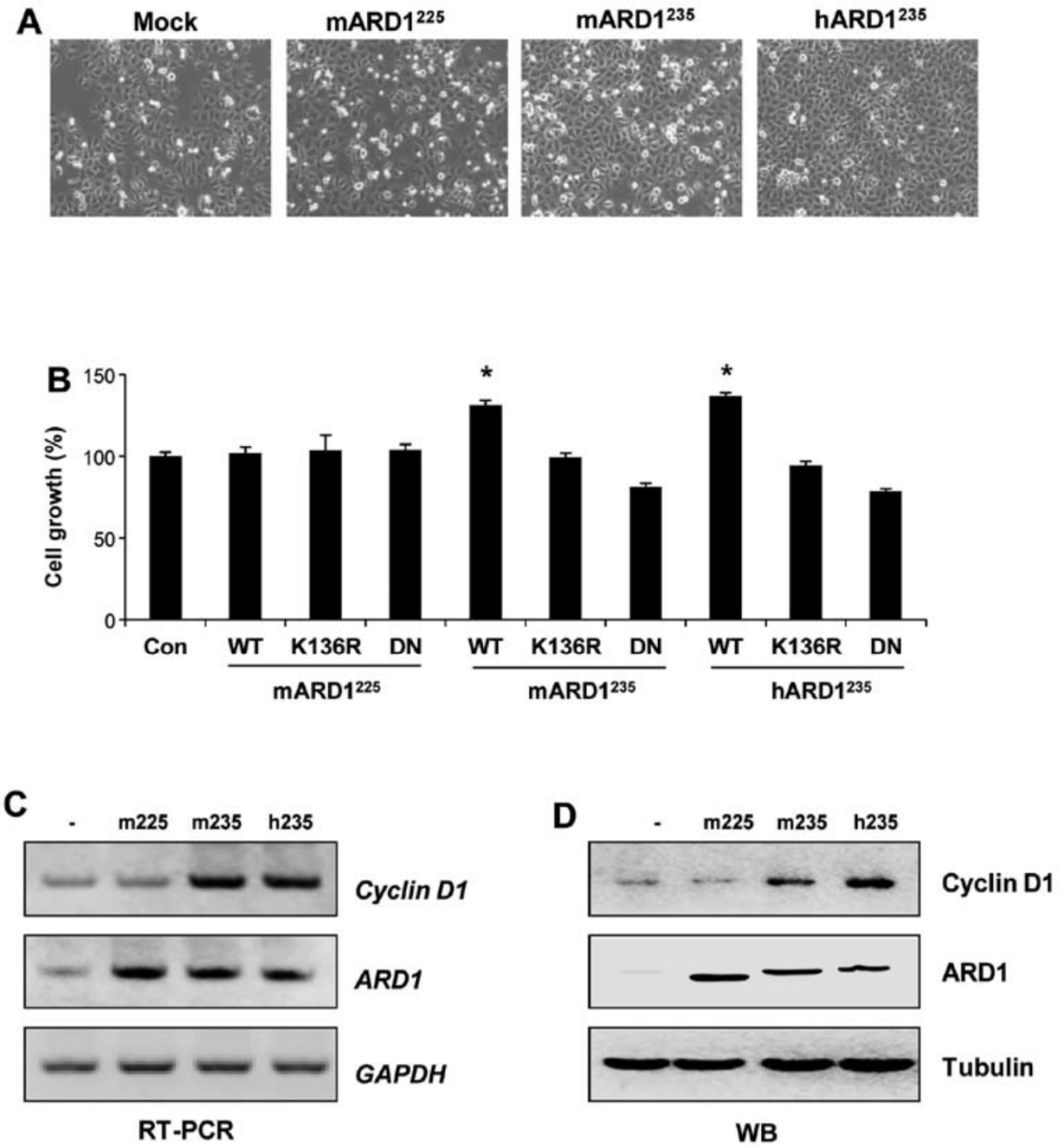


Figure 5. Autoacetylation of mARD1$^{235}$ and hARD1$^{235}$ but not mARD1$^{225}$ promotes cell proliferation under normoxic conditions. (A) HeLa cells were transfected with plasmids for ARD1 variants, then grown for 3 days and photographed. (B) After transfection of plasmids for wild-type and mutant ARD1 variants, cell growth was analyzed. *P<0.05 versus control. (C) HeLa cells were transfected with GFP-tagged mARD1$^{225}$, mARD1$^{235}$, and hARD1$^{235}$. The mRNA expression level of *cyclin D1* was then analyzed by RT-PCR. (D) The expression level of cyclin D1 protein from HeLa cells expressing ARD1 variants was analyzed by western blot analysis using an anti-cyclin D1 antibody.

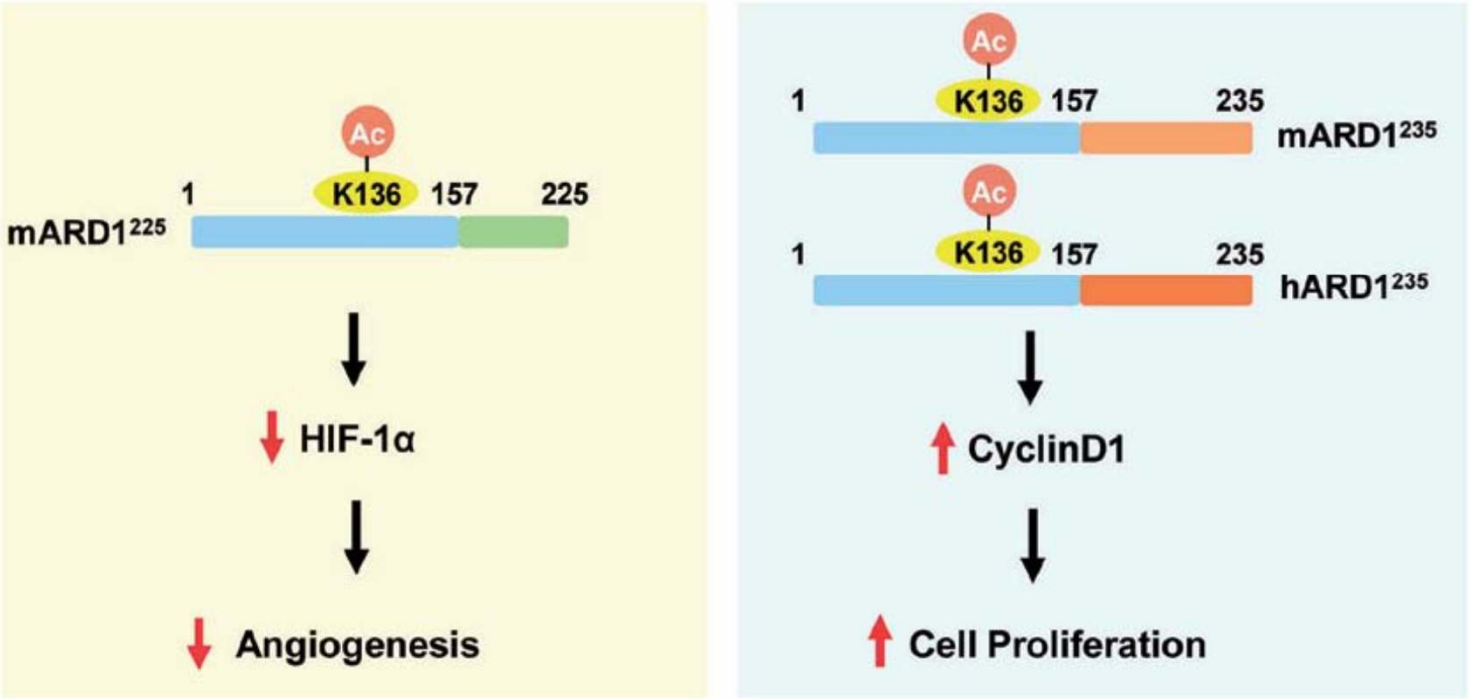


Figure 6. Isoform-specific roles of ARD1 autoacetylation in tumorigenesis. mARD1$^{225}$ autoacetylation inhibits angiogenesis through increased degradation of HIF-1α under hypoxic conditions. Under normoxic conditions, autoacetylation of mARD1$^{235}$ and hARD1$^{235}$ promote cell proliferation by upregulating the expression of cyclin D1. Thus, autoacetylation of ARD1 variants differentially regulates angiogenesis and cell proliferation in an isoform-specific manner, depending upon the physiological condition.